Influence of Lipid/Peptide Hydrophobic Mismatch on the Thickness of Diacylphosphatidylcholine Bilayers. A ^{2}H NMR and ESR Study Using Designed Transmembrane α-Helical Peptides and Gramicidin A†

Maurits R. R. de Planque,*,‡ Denise V. Greathouse,§ Roger E. Koeppe II,§ Hartmut Schäfer,|| Derek Marsh,⊥ and J. Antoinette Killian‡

Department Biochemistry of Membranes, Center for Biomembranes and Lipid Enzymology, Institute of Biomembranes, Utrecht University, Padualaan 8, 3584 CH Utrecht, The Netherlands, Department of Chemistry and Biochemistry, University of Arkansas, Fayetteville, Arkansas 72701, Fakultät für Physik und Geowissenschaften, Universität Leipzig, Linnéstrasse 5, D-04103 Leipzig, Germany, and Abteilung Spektroskopie, Max-Planck-Institut für biophysikalische Chemie, D-37077 Göttingen, Germany

Received January 29, 1998; Revised Manuscript Received April 22, 1998

ABSTRACT: We have investigated the effect of a series of hydrophobic polypeptides (WALP peptides) on the mean hydrophobic thickness of (chain-perdeuterated) phosphatidylcholines (PCs) with different acyl chain length, using ^{2}H NMR and ESR techniques. The WALP peptides are uncharged and consist of a sequence with variable length of alternating leucine and alanine, flanked on both sides by two tryptophans, and with the N- and C-termini blocked, e.g., $FmAW_2(LA)_nW_2AEtn$. ^{2}H NMR measurements showed that the shortest peptide with a total length of 16 amino acids (WALP16) causes an increase of 0.6 Å in bilayer thickness in di-C_{12}-PC, a smaller increase in di-C_{14}-PC, no effect in di-C_{16}-PC, and a decrease of 0.4 Å in di-C_{18}-PC, which was the largest decrease observed in any of the peptide/lipid systems. The longest peptide, WALP19, in di-C_{12}-PC caused the largest increase in thickness of the series (+1.4 Å), which decreased again for longer lipids toward di-C_{18}-PC, in which no effect was noticed. WALP17 displayed an influence intermediate between that of WALP16 and WALP19. Altogether, incorporation of the WALP peptides was found to result in small but very systematic changes in bilayer thickness and area per lipid molecule, depending on the difference in hydrophobic length between the peptide and the lipid bilayer in the liquid-crystalline phase. ESR measurements with spin-labeled lipid probes confirmed this result. Because thickness is expected to be influenced most at the lipids directly adjacent to the peptides, also the maximal adaptation of these first-shell lipids was estimated. The calculation was based on the assumption that there is little or no aggregation of the WALP peptides, as was supported by ESR, and that lipid exchange is rapid on the ^{2}H NMR time scale. It was found that even the maximal possible changes in first-shell lipid length were relatively small and represented only a partial response to mismatch. The synthetic WALP peptides are structurally related to the gramicidin channel, which was therefore used for comparison. In most lipid systems, gramicidin proved to be a stronger perturber of bilayer thickness than WALP19, although its length should approximate that of the shorter WALP16. The effects of gramicidin and WALP peptides on bilayer thickness were evaluated with respect to previous ^{31}P NMR studies on the effects of these peptides on macroscopic lipid phase behavior. Both approaches indicate that, in addition to the effective hydrophobic length, also the physical nature of the peptide surface is a modulator of lipid order.

The ways in which proteins and lipids interact are of fundamental significance for membrane structure and function. Evidence is accumulating that the extent of hydrophobic matching between these two membrane constituents is important in such interplay. Hydrophobic mismatch may influence the activity of membrane proteins (*1*, *2*), drive the formation of lipid microdomains and the lateral segregation of proteins in biomembranes (*3*−*5*), and govern protein sorting in the secretion pathway (*6*).

On a molecular level, it can be expected that a membrane system will counteract an energetically unfavorable mismatch situation. Depending on the exact nature of the lipid−protein system, this could be achieved in a number of ways. Proteins or peptides could tilt or kink when their transmembrane hydrophobic length is too long to match the bilayer, thus reducing their effective length. In the reverse situation, a transmembrane helix could adopt a more extended conformation (*7*, *8*), or a nontransmembrane orientation (*9*). Protein

† This work was supported by The Netherlands Foundation for Chemical Research (SON) with financial aid from The Netherlands Organization for Scientific Research (NWO), by NIH Grant GM 34968 (to R.E.K. and D.V.G.), by NATO Grant CRG 950357, and by EMBO Fellowship ASTF 8778 (to M.R.R.d.P.).

* Corresponding author. Telephone: 31-30-2535512. Fax: 31-30-2522478. E-mail: m.r.r.deplanque@chem.uu.nl.

‡ Utrecht University.

§ University of Arkansas.

|| Universität Leipzig.

⊥ Max-Planck-Institut für biophysikalische Chemie.

S0006-2960(98)00233-5 CCC: $15.00
Published on Web 06/12/1998

aggregation is another possible reaction, when the protein hydrophobic length is both too long and too short, because it reduces the amount of water-exposed nonpolar surface area (*10*). Alternatively, the lipids could respond to both mismatch situations by ordering or disordering their acyl chains, as described in the 'mattress model' of Mouritsen and Bloom (*11*) or the model of Owicki et al. (*12*). A drastic disordering may even drive the formation of inverted nonbilayer lipid phases (*13*−*15*). Although each of these molecular rearrangements will have consequences for membrane characteristics, little is known about the guiding principles behind these adaptations.

To understand the possible effects of hydrophobic mismatch at a molecular level, it is necessary to carry out systematic studies on well-defined protein−lipid complexes. Model peptides present a suitable tool to gain insight into such molecular interactions because of their well-defined structure. Synthetic polyleucines and polyleucine/alanines, with terminally located charged residues to ensure a transmembrane orientation, have been used to study peptide−lipid interactions and the effects of hydrophobic mismatch (*7*, *8*, *16*, *17*). Also the antibiotic gramicidin A (gA)[1] has been extensively investigated as a model transmembrane peptide (reviewed in *18*). In its channel conformation, gA spans the membrane as a $\beta^{6.3}$-helical dimer in which the N-termini are linked together by hydrogen bonding. The interfacially located C-termini of this dimer are rich in tryptophans and its core consists of hydrophobic residues. We chose to use related uncharged α-helical peptides (WALP peptides) which consist of a hydrophobic core with variable lengths of alternating leucine and alanine residues, flanked on both sides by tryptophans (see Table 1). These peptides were shown to form transmembrane α-helices in PC model membranes (*15*). Because single (*19*) as well as multiple (*20*−*23*) membrane-spanning proteins frequently display tryptophan residues near the membrane interface, WALP peptides are excellent models for α-helical transmembrane segments of these proteins.

In the present study, we focus on the possible shortening or stretching of the lipid acyl chains in bilayer systems that are confronted with a hydrophobic mismatch induced by transmembrane WALP peptides. Gramicidin was included for the purpose of comparison. Information about mean lipid acyl chain length was obtained from ^{2}H NMR quadrupolar splitting measurements using phospholipids with *sn*-2 perdeuterated chains. In addition, the interaction of the peptides with neighboring lipids was characterized by ESR measurements with lipid probes, spin-labeled in the fatty acid chain.

Data from both techniques indicate that the peptide hydrophobic length influences bilayer thickness in a systematic way such as to reduce the mismatch. The ESR measurements indicate that WALP peptides do not aggregate extensively in the bilayer, possibly due to the interfacial tryptophan residues of these peptides.

MATERIALS AND METHODS

Materials

The peptides WALP16, WALP17, and WALP19 (see Table 1) were synthesized as described before (*15*). The natural mixture of gramicidins from *Bacillus brevis* (gramicidin A′) was obtained from Sigma (St. Louis, MO). The *sn*-2 chain perdeuterated phospholipids 1,2-dilauroyl-*sn*-glycero-3-phosphocholine (DLPC-d_{23}), 1,2-dimyristoyl-*sn*-glycero-3-phosphocholine (DMPC-d_{27}), 1,2-dipalmitoyl-*sn*-glycero-3-phosphocholine (DPPC-d_{31}), and 1,2-distearoyl-*sn*-glycero-3-phosphocholine (DSPC-d_{35}) were synthesized based on the method of Boss et al. (*24*), using a modified procedure (*25*), or purchased from Avanti Polar Lipids Inc. (Birmingham, AL); both batches gave identical results. Deuterium-depleted water was from Isotec Inc. (Miamisburg, OH). 5-, 12-, and 14-(*N*-oxy-4,4-dimethyloxazolidin-2-yl)-stearic acids (5-, 12-, and 14-SASL) were synthesized according to Hubbell and McConnell (*26*).

Methods

NMR Sample Preparation. Peptides were incorporated into bilayers of *sn*-2 chain perdeuterated phospholipids by adding, at temperatures above the gel to liquid-crystalline phase transition, TFA-pretreated peptide dissolved in 0.5 mL of TFE to 0.5 mL of a lipid suspension in distilled water, followed by addition of 10 mL of water and immediate lyophilization (*15*). Lyophilized samples containing 10−20 μmol of *sn*-2 perdeuterated lipid and 3.3 mol % peptide were rehydrated in 1 mL of deuterium-depleted water. The samples were spun down at 30000*g* for 15 min at 4 °C, and the supernatant was removed. The pellet was washed with deuterium-depleted water, if the pH of the supernatant was below pH 6.

NMR Measurements. ^{2}H NMR spectra were recorded on a Bruker MSL 300 NMR spectrometer, using a high-power probe with a 7.5-mm solenoidal sample coil. The sample temperature was regulated to within ±0.5 °C, using a Bruker B-VT1000 temperature controller. ^{2}H NMR measurements were performed at 46.1 MHz, using a quadrupolar echo sequence (*27*) with a 2.6 μs 90° pulse, a 50 μs pulse separation, a repetition rate of two acquisitions per second, and a spectral width of 417 kHz, with 2048 data points in the time domain; 30 000−60 000 scans were accumulated. The free induction decays were left-shifted to begin at the top of the echo, zero-filled to 8192 points, and multiplied with an exponential window function equivalent to a line broadening of 50 Hz. Proton-decoupled ^{31}P NMR experiments were carried out at 121.5 MHz, with a 17 μs 90° pulse, a 1.3 s interpulse time, and gated proton-noise decoupling. A sweep width of 25 kHz, 1024 data points, and a 100 Hz line broadening were used, and approximately 8000 scans were acquired. Spectra were recorded at 10 °C above the gel-to-liquid-phase transition temperature of the pure lipids. At these relative temperatures, the physical characteristics of bilayers are expected to be most comparable (*28*).

Analysis of the ^{2}H NMR Spectra. Unsymmetrized ^{2}H NMR powder spectra were dePaked by nonnegative least-

[1] Abbreviations: NMR, nuclear magnetic resonance; ESR, electron spin resonance; Fm, formyl; Etn, ethanolamine; TFA, trifluoroacetic acid; TFE, trifluoroethanol; WALP, tryptophan-alanine-leucine peptide $FmAW_2(LA)_nW_2AEtn$; gA, gramicidin A; PC, phosphatidylcholine; DLPC, 1,2-dilauroyl-*sn*-glycero-3-phosphocholine; DMPC, 1,2-dimyristoyl-*sn*-glycero-3-phosphocholine; DPPC, 1,2-dipalmitoyl-*sn*-glycero-3-phosphocholine; DSPC, 1,2-distearoyl-*sn*-glycero-3-phosphocholine; DOPC, 1,2-dioleoyl-*sn*-glycero-3-phosphocholine; *n*-SASL, *n*-(*N*-oxy-4,4-dimethyloxazolidin-2-yl)stearic acid spin-label; H_{II}, inverse hexagonal lipid phase.

squares analysis with Tikhonov regularization (*29*). This procedure results in spectra that would be obtained for an aligned membrane with its bilayer normal parallel to the magnetic field. This enhances the resolution and results in doublets with splittings, $\Delta\nu_Q$, that relate to the bond order parameter $S_{CD}(i)$ according to

$$\Delta\nu_Q = \frac{3}{2}\frac{e^2qQ}{h}S_{CD}(i) \quad (1)$$

where $e^2qQ/h = 167$ kHz is the static quadrupolar coupling constant for a C$-^2$H bond (*30*). On the basis of geometric considerations, the values of $S_{CD}(i)$ are assumed to be negative; however, for practical reasons we will always refer to the absolute value. $S_{CD}(i)$ can be approximately related to the segmental order parameter $S(i)$ by assuming axial symmetry (*31, 32*):

$$S(i) = 2S_{CD2} \quad (2)$$

$$S(i) = 6S_{CD3} \quad (3)$$

for methylene and methyl C$-$D bonds, respectively.

Order parameter profiles were obtained by assuming that the segmental order varies monotonically along the acyl chain (*33*). The area of each resolved peak in the dePaked spectrum was calculated and, based on the ratio of this area to the total area of all peaks, assigned to a carbon position (*34*). The unresolved peak, which is associated to the plateau region, was fitted and subsequently deconvoluted into Gaussian peaks using the Origin Peak Fitting Module 3.5 from Microcal Software Inc. (Northampton, MA). The area and midpoint of these deconvoluted peaks were used for carbon assignment and $S(i)$ determination, respectively. The whole procedure was applied to both the negative and positive sides of the dePaked spectra, and the resulting values of $S(i)$ were averaged.

Estimation of Bilayer Thickness. The effective length of a saturated acyl chain in the liquid-crystalline phase of pure lipid bilayers has been found to be proportional to the average segmental order parameter $\langle S\rangle$ (*35, 36*). Under these conditions, the average length, $\langle L\rangle$, projected on the bilayer normal can be estimated from the relation (*37*):

$$\langle L\rangle = L_0\frac{1+\langle S\rangle}{2} \quad (4)$$

where L_0 ($= 1.27 \times n$ Å) is the projected length of an all-trans chain (1.27 Å is the projected distance between two carbon atoms in the all-trans state) and n is the number of C$-$C bonds between the third carbon and the methyl group of the *sn*-2 chain ($n = n_c - 3$). The hydrophobic bilayer thickness is then approximated by

$$\langle D\rangle = 2\langle L\rangle + 3.75 \text{ Å} \quad (5)$$

where 3.75 Å is the C$-$C distance, across the bilayer, between contacting terminal methyl groups, as determined by X-ray measurements (*38*). We applied this same procedure for bilayers with peptides incorporated.

The area per lipid molecule, A, was calculated according to (*37*) from the plateau region only:

$$A = \frac{86.9 \text{ Å}^2}{1+\langle S_p\rangle} \quad (6)$$

where $\langle S_p\rangle$ is the average order parameter in the plateau region, and $V_{CH2} = 27.6$ Å^3 is assumed for the volume of a CH_2 group in the fluid phase. It should be noted that alternative, simplified approaches are also regularly used for estimation of changes in bilayer thickness and lipid area (e.g., *37, 39*).

ESR Sample Preparation. Peptide dissolved in 0.5 mL of TFE was added to 0.5 mL of a 3.0 mM lipid solution in 1/1 chloroform/methanol, v/v, doped with 1 mol % 5-, 12-, or 14-SASL from a 3.3 mM methanol solution. The peptides were incorporated into bilayers by evaporation of the solvents on a rotavapor and subsequent hydration of the dry lipid/peptide film in 40 μL of distilled water, at temperatures above the gel to liquid-crystalline phase transition. Samples were spun down at 5000*g* for 15 min at room temperature in 1-mm i.d. capillaries, which were flame-sealed after removal of the supernatant. The method of ESR sample preparation deviated for practical reasons from ^{2}H NMR sample preparation, but both preparation methods yielded similar results with the latter technique (data not shown).

ESR Spectroscopy. ESR spectra were recorded on a Varian Century Line Series 9-GHz spectrometer equipped with a nitrogen gas flow-temperature regulation system. Sample-containing capillaries were accommodated within standard 4-mm quartz ESR tubes containing light silicone oil for thermal stability. Temperature was measured by a fine-wire thermocouple located at the top of the microwave cavity within the silicone oil. Conventional, in-phase ESR spectra were recorded at a modulation amplitude of 1.6 G p$-$p and a modulation frequency of 100 kHz, with a sweep width of the static field of 100 G.

RESULTS

^{2}H NMR Measurements. WALP peptides and gramicidin (Table 1) were incorporated at a 1/30 peptide/lipid molar ratio into bilayers of *sn*-2 chain perdeuterated DLPC, DMPC, DPPC, and DSPC. ^{31}P NMR measurements (see also *15*) confirmed that the lipids in these systems are in a bilayer organization (data not shown). The effect of the peptides on acyl chain order was characterized by ^{2}H NMR. Figure 1 presents, as an example, the ^{2}H NMR spectra of DLPC bilayer dispersions, with and without the different peptides. Spectra of the pure lipids are with regard to line shape (*40*) and quadrupolar splitting (*41, 42*) in good agreement with previous studies. Visual inspection of the spectra reveals peptide-specific increases in quadrupolar splittings for the central methyl and the outer methylene peaks, the latter representing the plateau region. This demonstrates that all the peptides order the DLPC chains, and that the order increases as a function of the length of the WALP peptides. The largest increases in order are observed for gramicidin and WALP19.

In these powder spectra, the individual methylene signals are not all completely resolved, which limits a detailed analysis of the data. Therefore, the spectra were transformed

Table 1: Amino Acid Sequences of the Peptides Used and Their Estimated Total Length[a]

peptide	sequence	length (Å)
WALP16	formyl-AWWLALALALALAWWA-ethanolamine	25.5
WALP17	formyl-AWWLALALALALALWWA-ethanolamine	27.0
WALP19	formyl-AWWLALALALALALALWWA-ethanolamine	30.0
gramicidin	formyl-VGALAVVVWLWLWLW-ethanolamine[b]	26.0[c]

[a] It is assumed that the WALP peptides are α-helical and that each amino acid contributes an axial length of 1.5 Å, with the C-terminal ethanolamine included as the length of an additional residue. [b] Underlined residues are D-amino acids. [c] For the $\beta^{6.3}$ dimer conformation (*78*, *79*).

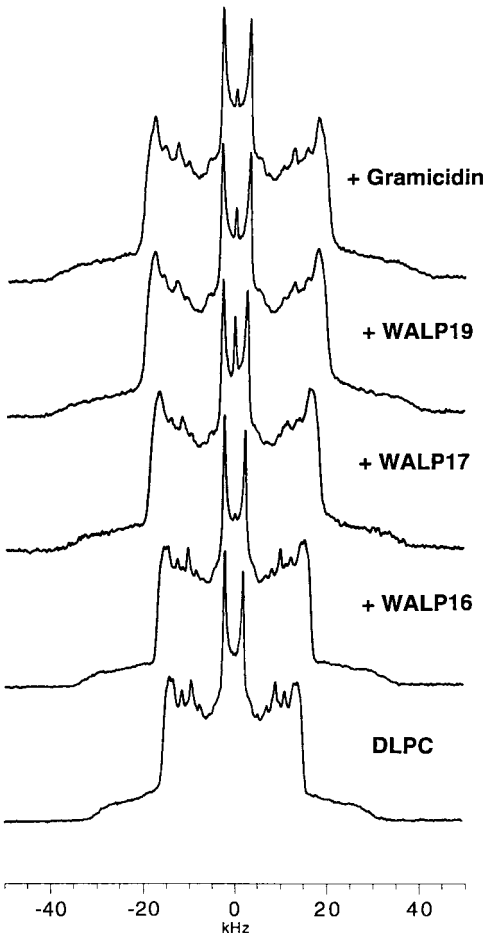

FIGURE 1: ^{2}H NMR spectra for peptide/DLPC-d_{23} dispersions at a 1/30 molar ratio and at 10 °C. Spectra are shown without peptide (DLPC) and for samples containing the peptides indicated.

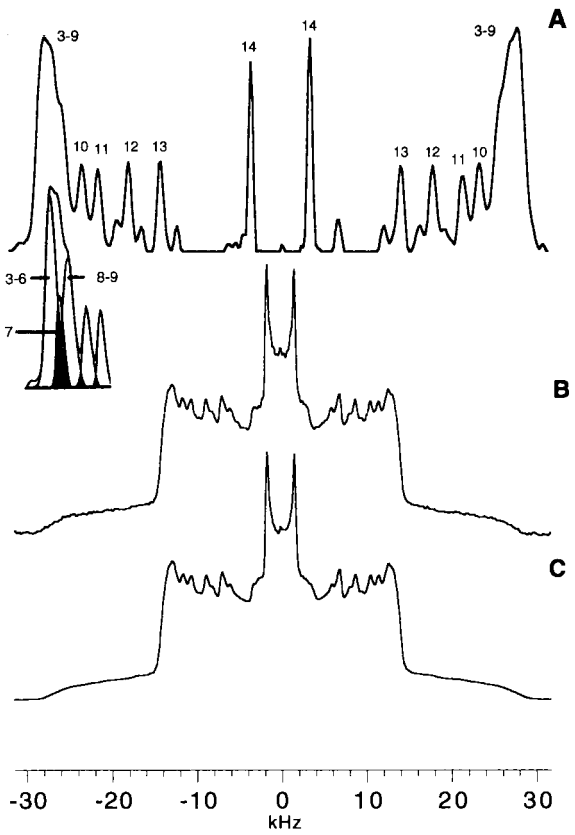

FIGURE 2: (A) DePaked ^{2}H NMR spectrum of WALP16/DMPC-d_{27} (1/30 molar ratio) at 34 °C. Peaks were assigned as described under Materials and Methods. The insert shows the assignment of the deconvoluted plateau peak, with the nonassigned peaks corresponding to chain positions 10 and 11. (B) ^{2}H NMR powder spectrum for the WALP16/DMPC-d_{27} system in (A). (C) Simulation of the powder spectrum of WALP16/DMPC-d_{27} in (B), by using the parameters derived from the dePakeing procedure in (A).

into oriented ones by means of the dePakeing procedure. An example is shown in Figure 2A, for a sample of DMPC with WALP16. The assignment of the resolved major peaks and of the plateau region, by the use of deconvolution, is also depicted in the figure. Additional minor peaks on both sides of 13 C−methylene correspond to the nonequivalent 2 C-atom deuterons of the *sn*-2 chain (*35*, *43*, *44*). The low-intensity signal near 7 kHz, present in all systems studied, was counterbalanced by an equisized negative peak around −7 kHz in a different dePakeing algorithm. Since this corresponds to the expected position of the shoulders of the methyl resonances, this signal was considered an artifact and was further ignored. Also shown is a comparison between the original ^{2}H NMR powder spectrum (Figure 2B) and the powder spectrum as recalculated from the dePaked version (Figure 2C). The accurate match of original and recalculated spectra underlines the reliability of the dePakeing procedure that was applied.

For all peptide/lipid systems, segmental order parameters, $S(i)$, were obtained from the dePaked spectra, and the resultant order parameter profiles are depicted in Figure 3. The pure lipids are characterized by the familiar plateau region of relatively high chain order near the lipid headgroups, followed by a second part of the profile that declines rapidly toward the low order of the methyl moiety in the core of the bilayer. The segmental order parameters that are obtained here are in agreement with the available literature data on the order of pure lipids (*35*, *43*, *45*). The longer lipids show a decreased order parameter in the plateau region, relative to the shorter ones, again in agreement with previous studies (*45*, *46*). Longer WALP peptides always induce higher order than do the shorter ones, and the effect of gramicidin exceeds that of the longest WALP analogue, except in DSPC. The results obtained with gramicidin are comparable with previous studies (*47*, *48*). In DLPC and DMPC, all peptides are characterized by chain order profiles

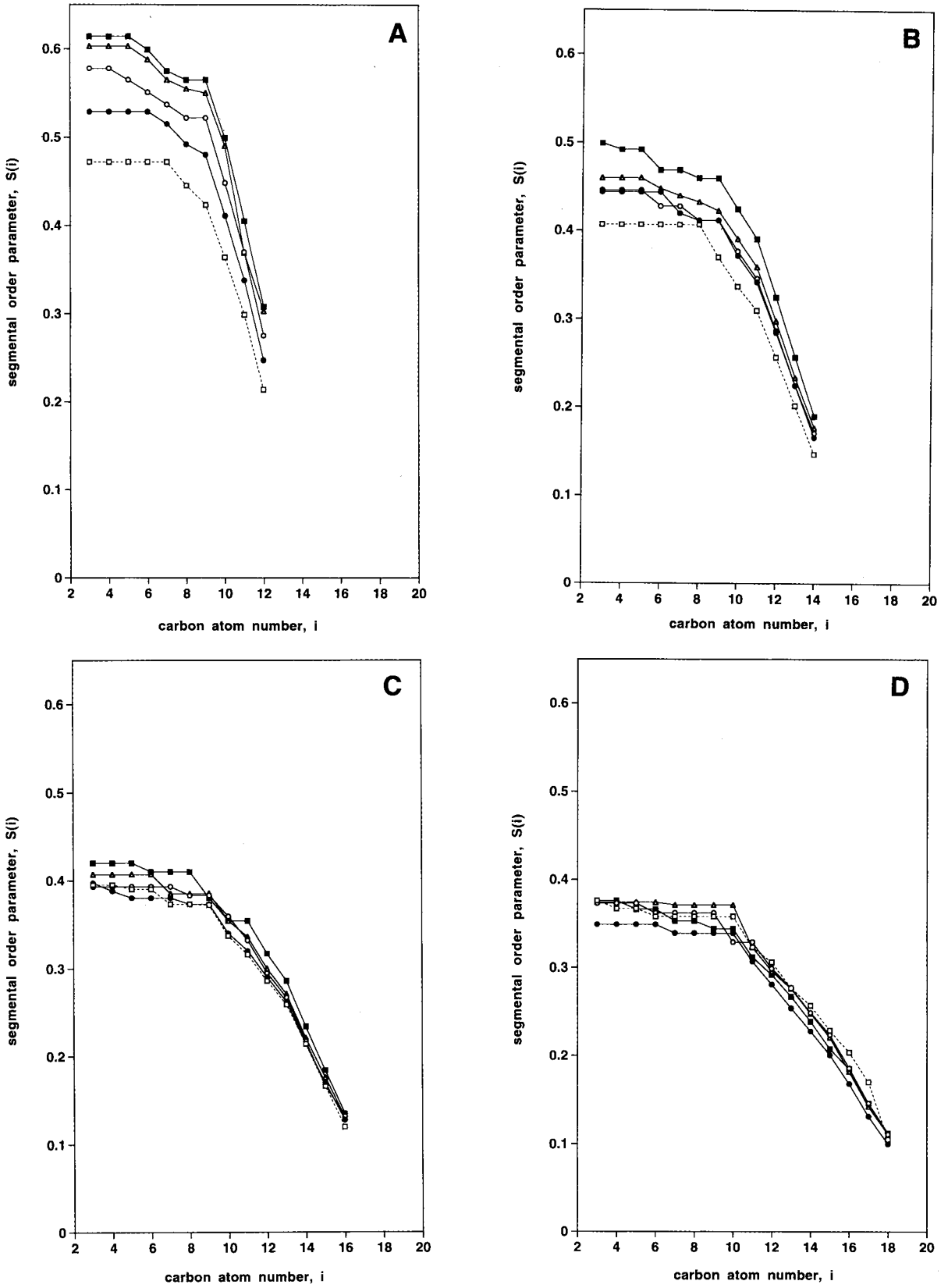

FIGURE 3: Experimental order parameter profiles of the dePaked ^{2}H NMR spectra of *sn*-2 chain perdeuterated phosphatidylcholines. (A) DLPC at 10 °C, (B) DMPC at 34 °C, (C) DPPC at 51 °C, and (D) DSPC at 65 °C, respectively: pure lipid (□), with WALP16 incorporated (●), with WALP17 (○), with WALP19 (△), and with gramicidin (■). Methods used for deriving the order profile are described under Materials and Methods.

that lie entirely above the chain profile of the pure lipid, suggesting that an increase in bilayer thickness is induced by the peptides. The DLPC profiles, however, have larger separations from the pure lipid profiles than do the corresponding ones for DMPC. This demonstrates that the DMPC membrane is somewhat less influenced by the peptides than

Table 2: Estimated Hydrophobic Bilayer Thicknesses (Å) and in Parentheses Area per Lipid Molecule (Å^2) of Pure Lipid, and Changes in Hydrophobic Thickness and Area per Molecule Relative to Pure Lipids, for Systems at a 1/30 Molar Ratio of Peptide to Lipid[a]

	DLPC	DMPC	DPPC	DSPC
pure lipid	19.9 (59.2)	22.5 (61.8)	25.4 (62.8)	28.5 (63.6)
+WALP16	+0.6 (−1.9)	+0.4 (−1.1)	+0.0 (+0.1)	−0.4 (+1.1)
+WALP17	+1.0 (−3.2)	+0.4 (−1.2)	+0.1 (−0.3)	−0.1 (+0.0)
+WALP19	+1.4 (−4.6)	+0.6 (−1.7)	+0.2 (−0.6)	+0.0 (−0.3)
+gramicidin	+1.5 (−4.8)	+1.0 (−2.9)	+0.4 (−1.2)	−0.2 (+0.3)

[a] Measurements were performed at 10 °C above the main phase transition temperature of the pure lipids, these being 10, 34, 51, and 65 °C for DLPC, DMPC, DPPC, and DSPC, respectively. The estimated experimental precision in hydrophobic thickness is ±0.1 Å.

is the membrane composed of DLPC lipids. With the longer chain lipids, the perturbations in chain order become relatively small, and the profiles for the different peptides cross each other more often. This is clearly observed with DPPC and DSPC, where the profiles with the WALP peptides may even remain below those of the pure lipids, indicating that a decrease in membrane thickness is induced by these peptides.

The mean hydrophobic thicknesses of the different lipid/peptide systems were estimated from the segmental order parameters, $S(i)$, according to Nagle (*37*), as described under Methods. These values are presented in Table 2. The hydrophobic membrane thicknesses obtained for the pure lipid systems are in fairly good agreement, within about 1 Å, with values based on X-ray measurements (*49*, *50*). We will focus first on the effects induced by the WALP peptides. In DLPC, all of these peptides cause a systematic increase in the estimated membrane thickness relative to the pure lipid. The largest effects of the whole study were observed in DLPC, with an estimated increase in thickness of 1.4 Å for WALP19. A systematic increase with increasing peptide length is also observed, but to a lesser extent, in DMPC systems. In DPPC, a slight increase or no change in thickness upon incorporation of WALP peptides is obtained. In the longest lipid, DSPC, the incorporation of WALP19 has no effect, and the shorter WALP16 and WALP17 even cause a slight decrease in thickness relative to the pure DSPC bilayer. The maximum decrease amounts to −0.4 Å for WALP16 in DSPC. Thus, different WALP analogues (that differ only in hydrophobic length) in the same lipid cause a systematic, length-dependent disturbance of average bilayer thickness. Also when comparing the effects of one particular WALP peptide in lipids of different length, a systematic decrease from stretching to shrinking upon increasing chain length is observed. The changes in mean area per lipid molecule calculated solely from the plateau values of the chain order parameters (see Methods) are also given in Table 2. These changes are seen to be conjugate to those in the lipid length and are a further manifestation of hydrophobic matching.

With gramicidin, a similar systematic decrease from stretching to shrinking was seen for the series of lipids of different lengths. Although not the longest peptide assembly (Table 1), the 26-Å-long gramicidin dimer exerts the largest perturbing influence in most of the PC-lipids, except in DSPC, where the effect of gramicidin is intermediate between

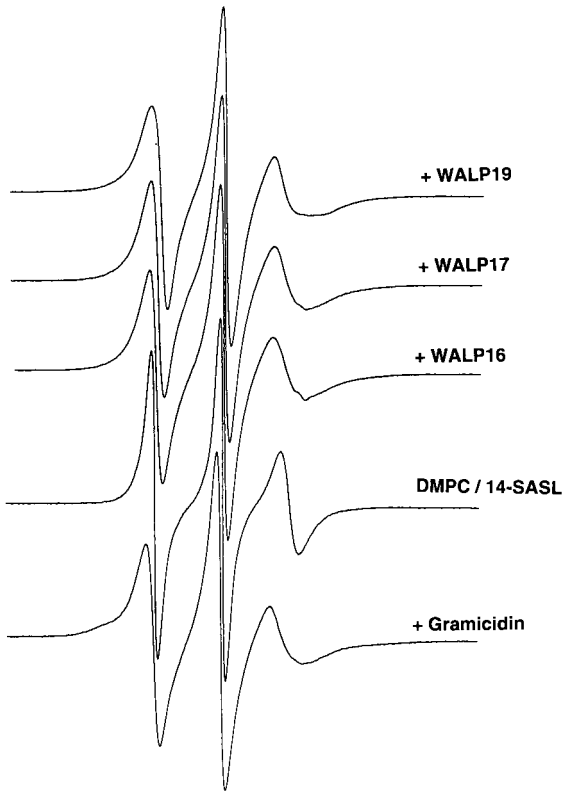

FIGURE 4: ESR spectra of the 14-SASL stearic acid spin-label in DMPC, in the absence and in the presence of the peptides indicated, at a peptide/lipid molar ratio of 1/10 and 34 °C, total scan width = 100 G.

that of WALP16 (∼25.5 Å) and WALP17 (∼27 Å). We note, however, that the structural features are significantly different when comparing gramicidin with the WALP peptides, and the results suggest that another factor in addition to the hydrophobic length plays a secondary role (see Discussion).

ESR Measurements. ESR spectra obtained from spin-labeled lipids provide information on the dynamics and conformational order of lipids through the line widths, line shapes, and hyperfine splittings of the 'fluid' or bulk lipid component (*51*). Peptide assemblies that specifically restrict the lipid acyl chains in their rotational motion cause a second or 'restricted' spectral component to appear, which can be related to the peptide aggregational state (*52*, *53*). ESR experiments were performed with different lipid/spin-label combinations, of which DMPC and the 14-SASL spin-label at 34 °C potentially present the optimal resolution of such two-component spectra. For comparison with the ^{2}H NMR experiments, samples were first prepared with a 1/30 molar ratio of peptide to lipid. The resultant spectra were very similar to those of the pure lipid (data not shown), and apparently overall lipid dynamics were not severely affected at this ratio, relative to the intrinsic line widths in the absence of peptide. The peptide concentration was therefore increased to 10 mol %, at which ratio DMPC systems still maintain a planar bilayer organization (*15*), yielding the spectra depicted in Figure 4.

Pure DMPC with 14-SASL is characterized in the fluid lamellar phase by a spectrum with three sharp, symmetrical, quasi-isotropic peaks. Substantial changes in both line shape and anisotropy of the hyperfine splitting were observed upon

incorporation of the WALP peptides. However, even at this relatively high peptide/lipid molar ratio (1/10), there is no evidence for a second, more motionally restricted spin-labeled lipid component, such as is generally observed for the 14-C atom spin-labels with large integral proteins or oligomeric transmembrane peptides (*54*, *55*). In contrast, a second, motionally restricted component is observed in the outer wings of the central three-line component (which corresponds to the fluid lipid population), in gramicidin/DMPC complexes at a 1/10 molar ratio. This second component is more readily detected in the low-field region of the gramicidin/DMPC spectrum and is absent from the spectra of the samples containing the WALP peptides. The direct motional restriction of the lipid chains by gramicidin has been observed previously (*56*−*58*). The inference that can be drawn from these results with the 14-C atom spin-labeled lipids in the reconstituted lipid membranes is that the WALP peptides are most probably present as monomeric transmembrane helices, and certainly are not present as extensive oligomers. Other combinations of lipids, peptides, and 14-, 12-, and 5-SASL spin-label positional isomers indicated that even under more extreme conditions of mismatch no substantial aggregation of these particular peptides occurred.

The WALP peptides therefore affect the lipid chain mobility in a generalized fashion throughout the membrane, as recorded by the 14-C atom spin-labels. Under these circumstances, the perturbations in chain mobility can be recorded more readily from the ESR spectra of spin-labels that are attached at the 5-C atom of the chain. This is because, being situated closer to the lipid polar headgroups, the spectra from such 5-SASL spin-labels display a very well-defined axial anisotropy. These ESR spectra are given in Figure 5, for DMPC in the fluid phase with the different WALP peptides. The outer hyperfine splitting ($2A_{max}$) is increased in a systematic way by the peptides of increasing length, and correspondingly the apparent inner hyperfine splitting ($2A_{min}$) is decreased. The values for the apparent hyperfine splittings, for both the 5-SASL and 14-SASL spin-labels, are listed in Table 3. Also included in Table 3 are values for the increase in effective spectral anistropy, Δ-($A_{max} - A_{min}$), that is induced by the peptide. The latter increases systematically with peptide length and parallels rather closely the length dependence of the peptide-induced changes in quadrupolar splittings that are observed by ^{2}H NMR (cf. Figure 3 and Table 2). In the case of the spin-labeled lipids, however, the effective hyperfine anisotropy is determined not only by the chain order, but also includes contributions from motional rates that are slow on the spin-label ESR time scale (see *59*, *60*). It is likely that the peptides not only increase the chain order in DMPC, but also slow the rates of certain rotational components, conceivably to different extents for WALP peptides and for gramicidin.

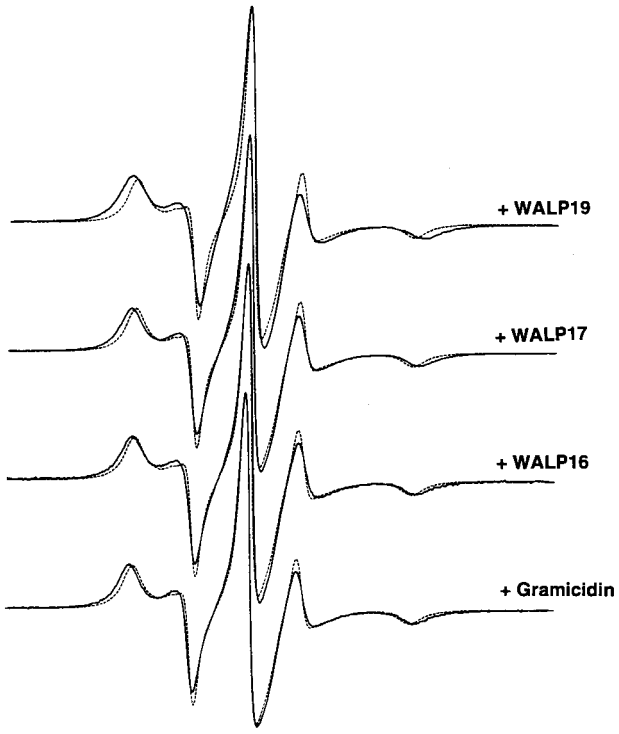

FIGURE 5: ESR spectra of the 5-SASL stearic acid spin-label in DMPC in the presence (continuous line) and in the absence (dotted line) of the peptides indicated, at a peptide/lipid molar ratio of 1/10, at 34 °C, total scan width = 100 G.

DISCUSSION

In this study, we investigated by ^{2}H NMR and ESR spectroscopy if and how incorporation of transmembrane peptides into model membranes influences the lipid chain conformations and mean bilayer thickness as a consequence of hydrophobic mismatch. In addition, the combination of these two techniques offers, via the well-defined length variations in the set of WALP peptide analogues, the opportunity to gain insight into length adaptations of lipids in direct contact with a mismatching peptide. The ESR data additionally serve a second aim in providing information on potential peptide aggregation, which would be another possible way to relieve mismatch-imposed constraints. Finally, the information obtained on changes in apparent bilayer thickness can be related to data previously obtained on hydrophobic mismatch from studying lipid phase behavior (*15*).

Effects of Peptides on Average Bilayer Thickness. The notion that, also in the presence of peptides, order parameters can be used to estimate the bilayer thickness is supported by the similar shape of the chain order profiles in the presence of gramicidin and WALP peptides to those in the absence of peptides (Figure 3), thus excluding gross, qualitative peptide-induced local perturbations in the chain order profile. ^{2}H NMR as well as ESR results showed that WALP peptides do induce clear effects on bilayer thickness, and that these effects are directly correlated with the extent of hydrophobic mismatch (Table 2). Conjugate to these changes in mean bilayer thickness, there are compensating changes in the effective mean area per lipid molecule (see Table 2). This is expected, since a lipid bilayer is effectively 'incompressible' with respect to volume changes (*61*). In DLPC and DMPC (see also Table 3), the longer WALP peptides proved to be more potent lipid 'stretchers' than the shorter ones, whereas in DSPC the shorter WALP peptides were more effective 'shrinkers'. These systematic effects were strongest in DLPC, and support unambiguously the notion that hydrophobic mismatch between a transmembrane peptide and its lipid environment leads to a bilayer response that reduces the extent of mismatch (*11*, *15*, *62*). The results obtained with gramicidin were consistent with previous ^{2}H

Table 3: Outer ($2A_{max}$) and Inner ($2A_{min}$) Hyperfine Splittings (G) from the ESR Spectra of 5-SASL and 14-SASL Lipid Spin-Labels in Peptide/DMPC Systems at 1/10 Molar Ratio and 34 °C[a]

	5-SASL			14-SASL		
	$2A_{max}$	$2A_{min}$	$\Delta(A_{max} - A_{min})$	$2A_{max}$	$2A_{min}$	$\Delta(A_{max} - A_{min})$
DMPC	50.1	19.0	0	32.1	25.3	0
+WALP16	52.1	18.8	1.1	33.3	23.8	1.3
+WALP17	52.6	18.3	1.6	33.6	22.8	2.0
+WALP19	53.4	17.8	2.3	34.1	22.3	2.5
+gramicidin	52.1	18.8	1.1	42.6/33.6[b]	22.6	(2.1)

[a] Values are also given for the increases in effective hyperfine anisotropy, $\Delta(A_{max} - A_{min})$, relative to DMPC alone. The precision in measurement of hyperfine splittings is 0.1 G. [b] Estimated outer hyperfine splittings for the restricted and fluid components, respectively.

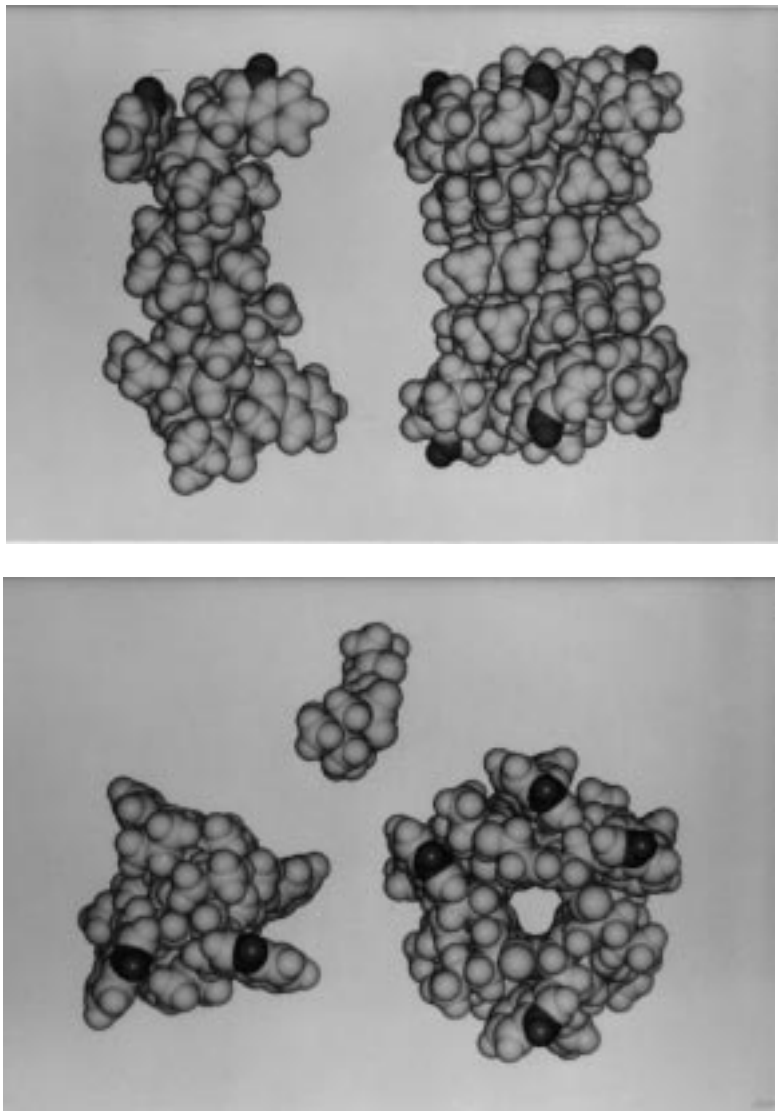

FIGURE 6: Side view (top panel) and top view (bottom panel) of WALP17 (left), gramicidin (right), and an all-trans diacylphosphatidylcholine (middle). When comparing both panels, please note that the top view is on a 3% smaller scale as the side view. Tryptophans are visible as protruding rings near the termini of both peptides, with front-turned indole NH-groups darkened.

NMR (*47*, *48*) and ESR (*57*, *58*) studies, and in general proved coherent with the results obtained with the synthetic peptides. However, in most lipids, except in DSPC, gramicidin displayed a bilayer-perturbing influence that was much more potent than a WALP peptide of the same length. The gramicidin β-helical dimer differs from a WALP α-helical monomer in shape, cross-sectional area, and number of tryptophans that are present at the interface (see Figure 6). Some of these factors—in addition to hydrophobic length—are likely to modulate the lipid-perturbing influence of the peptides. Nevertheless, the primary and most important factor is the mismatch between lipid and embedded peptide. Within the family of WALP peptides, the length correlation is very good.

Overall Extent of Lipid Adaptation. Although the total length of the peptides is known or can be estimated (Table 1), it is not known what exactly determines their effective hydrophobic length. Because tryptophans display a strong interaction with especially the interfacial region of a membrane (*63*), their positioning within the molecule may be an

important factor in defining the length of the membrane spanning region. Quantitative analysis of hydrophobic mismatch thus becomes feasible by comparing the effects of peptides with well-defined variations in hydrophobic length. The three WALP analogues differ only in the number of central residues, the contribution of which to the total length can be expected to be about 1.5 Å per amino acid residue in an α-helical conformation. As is evident from Table 2, the differences in peptide length were not reflected in an equisized increase or reduction in calculated average membrane thickness. In other words, a complete lipid adaptation to the imposed mismatch could not be accounted for by the data on mean lipid length obtained from ^{2}H NMR. However, the data measured are averages over all lipids, because of the long time scale of ^{2}H NMR relative to lipid translational diffusion times. It is generally assumed that lipids further away from a membrane-perturbing protein or peptide will be influenced to a lesser extent than lipids that are in direct contact with it (*11*, *62*, *64*, *65*). From a mismatch point of view, the behavior of these 'first-shell' lipids is expected to be most affected and to be directly related to the absolute hydrophobic length of the peptide.

Adaptation of Lipids in Direct Contact with Peptides. To test whether the first-shell lipids could display a complete response to a mismatch situation in the presence of WALP peptides, it is necessary to specify the number of these lipids per peptide, a parameter that is related to the peptide aggregational state. In our model, we therefore made use of the assumption, that is supported by ESR, that the peptides are dispersed as monomers or at most as dimers (see below). Based on geometrical considerations, the number of acyl chains that are in direct contact with a WALP monomer or dimer will be approximately 20 or 28, respectively (*52*). This corresponds to a number of first-shell diacyl lipids (N_1) of $N_1 = 10$ for a monomer or $2N_1 = 14$ for a dimer. Under the experimental conditions used, the total number of lipids per peptide (N_t) is 30, and all 'bulk' lipid will be present in the second and third shells, when the peptides are homogeneously dispersed. The maximum possible extent of stretching of the first-shell lipids can be estimated by assuming that they alone are responsible for the effects on chain order, while the other lipids remain unperturbed. With rapid translational averaging over all diffusing lipids, the mean segmental order parameter, $\langle S\rangle_1$, of the first-shell lipids is related to the average, $\langle S\rangle$, over all lipids, which is the experimentally determined quantity, by

$$\langle S\rangle_1 = (\langle S\rangle - \langle S\rangle_0)\frac{N_t}{N_1} + \langle S\rangle_0 \qquad (7)$$

where $\langle S\rangle_0$ is the mean segmental order parameter for all remaining lipids, outside the first shell, which is equivalent to the experimentally obtained value of $\langle S\rangle$ for a pure lipid system. The averaged projected length, $\langle L\rangle_1$, of the first-shell lipids is then obtained by substituting $\langle S\rangle_1$ from eq 7 for $\langle S\rangle$ in eq 4. The upper limit values for first-shell lipid adaptation obtained in this way (Table 4) are considerably larger than the experimentally derived mean values (cf. Table 2).

Figure 7 shows the estimated maximum possible hydrophobic thickness of the bilayer shell immediately adjacent to the different monomeric peptides, based on the values in Tables 2 and 4, as compared to the thickness of the pure lipid bilayers in the liquid-crystalline phase and in the all-trans state, where in the latter case the lipids are stretched to their maximum. Also shown in the figure are the estimated total lengths of the three WALP peptides (dashed lines). Figure 7 summarizes the most important observations: (1) the longest peptide induces the highest increase in bilayer thickness in the short lipids, and the shortest

Table 4: Estimated Maximum Possible Increases in Hydrophobic Bilayer Thicknesses (Å), Relative to Pure Lipids, of First-Shell Lipids, Calculated for Monomeric WALP Peptides and for a Dimeric Aggregational State of the WALP Peptides and Gramicidin

	DLPC	DMPC	DPPC	DSPC
		Monomer		
+WALP16	+1.7	+1.2	+0.0	−1.3
+WALP17	+2.9	+1.3	+0.4	−0.2
+WALP19	+4.3	+1.8	+0.7	+0.0
		Dimer		
+WALP16	+2.4	+1.7	+0.0	−1.8
+WALP17	+4.1	+1.8	+0.6	−0.3
+WALP19	+6.1	+2.6	+0.9	+0.0
+gramicidin[a]	+6.3	+4.3	+1.8	−0.7

[a] One transmembrane gramicidin channel can be compared with a dimeric side-by-side WALP aggregational state because the cross-sectional area of both assemblies should be approximately equal.

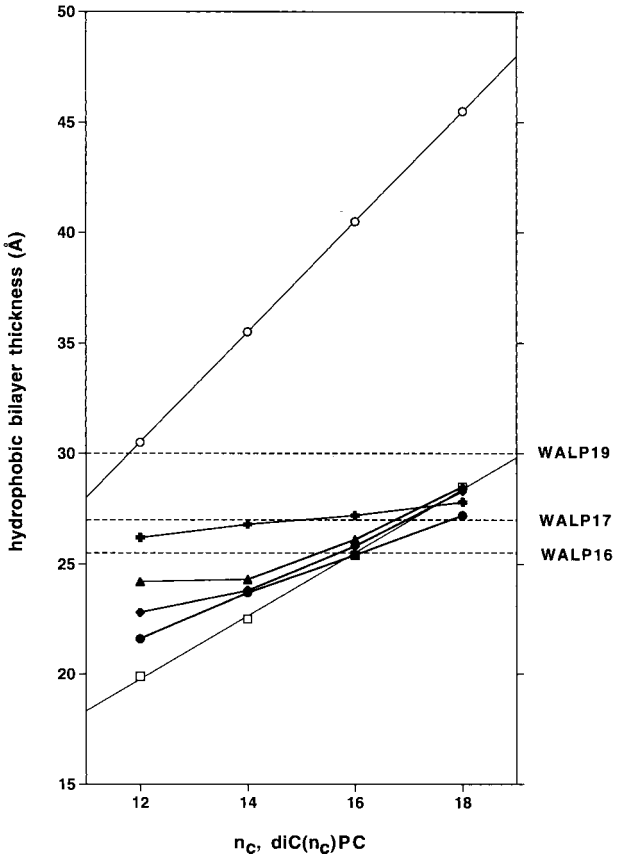

FIGURE 7: Calculated maximum effective hydrophobic bilayer thickness of the first-shell lipids surrounding monomeric WALP16 (●), WALP17 (◆), and WALP19 (▲) peptides, and the $\beta^{6.3}$ gramicidin channel (+) in di-C(n_c)-PCs as a function of lipid chainlength, n_c. Also given are the effective hydrophobic thicknesses of di-C(n_c)-PC bilayers in the absence of peptide (□) and the predicted hydrophobic bilayer thicknesses for all-trans chains (○). The measurement temperature is 10 °C above the chain-melting transition temperature in each case. The calculated total lengths of the α-helical WALP peptides are indicated by the horizontal lines.

peptide induces the largest shrink in the longer lipids; (2) for WALP16, the values apparently correspond with fully matching lipid chains in DPPC and for WALP17 with a notional di-C_{17}-PC, while WALP19 seems to have the best match with DSPC; (3) even in DLPC, where the largest stretch is observed, the adaptations are small compared to the all-trans length and they are less than the total length of the peptides; (4) the adaptations are also less than the relative differences in hydrophobic length between the various peptides; (5) in the presence of the different peptides, the first-shell bilayer thickness is less dependent on chain length than in the pure lipid systems, illustrating the acyl chain adaptation to the hydrophobic mismatch; and (6) for gramicidin, the first-shell bilayer thickness is less dependent on chain length than for the WALP peptides, suggesting that gramicidin induces a more complete lipid adaptation to mismatch, which may reflect the greater rigidity of this peptide. This is also consistent with the results of Goulian et al. (*66*), who showed that increasing tension on DOPC membranes modulates the mismatch in hydrophobic thickness between a gramicidin dimer and the membrane, but that the effect is much weaker on channel lifetime than on formation rate. The results suggested that the lipid/peptide hydrophobic matching is less than complete (as we show in Figure 7), and, importantly, that the dimer, once formed, is relatively rigid.

All these conclusions also hold if it is assumed that the WALP peptides are dimeric, in calculating the first-shell bilayer thickness. It should be noted, that with probably more realistic assumptions in which the second- and third-shell lipids are also adapted, but by 25 or 50% less than the first-shell lipids, the changes with respect to the mean data are considerably smaller in all systems (calculations not shown). Thus, assuming monomeric or dimeric peptide aggregation, it can be concluded that the lipids adjacent to a mismatching WALP peptide display only a partial adaptation to the hydrophobic mismatch.

Aggregation State of the Peptides. Insight into the aggregational state of the peptides was obtained by ESR measurements, which showed that the lipid chains spin-labeled on the C-14 atom are not specifically restricted by interaction with the transmembrane WALP peptides. The reason for this most probably lies in the fact that the average cross-sectional area of a single transmembrane α-helix is not appreciably larger than that of a fluid phospholipid molecule. Therefore, an isolated α-helix does not provide the extensive intramembranous hydrophobic surface that is presented to the lipid chains by large integral proteins or transmembrane peptide oligomers. It should be noted that at the high peptide/lipid ratios used for the ESR measurements, most monotopic proteins will relatively easily form aggregates (see, e.g., *53*). Only one unambiguous case has been reported of a peptide being present as an isolated transmembrane helix under these conditions. This is the L37A mutant of phospholamban in its monomeric form, which nevertheless was found to directly restrict the rotational motion of spin-labeled lipid chains (*67*). On the other hand, the highly hydrophobic lung surfactant protein SP-C, which is thought to cross the membrane as a single α-helix, does not evidence a second motionally restricted spin-labeled lipid population (*68*), similar to the situation with the WALP peptides in the present study. Although the exact reason for these differences in peptide behavior is not known, the absence of the motionally restricted spin-labeled lipid population in the presence of high concentrations of WALP peptides strongly indicates that these peptides are not aggregated and are present as monomers, or at most dimers, in the reconstituted systems (see Note Added in Proof). The experiments with gramicidin under identical reconstitution conditions serve as a control that such a motionally restricted lipid population should readily be detectable if it were present with the WALP peptides (see Figure 4).

Table 5: Phases of Peptide/Lipid Combinations Used at a 1/10 Molar Ratio of Peptide to Lipid[a]

	DLPC	DMPC	DPPC	DSPC
+WALP16[b]	bilayer	bilayer	bilayer[d]	H_{II}
+WALP17[b]	bilayer	bilayer	isotropic	H_{II}
+WALP19[b]	bilayer	bilayer	bilayer	isotropic
+gramicidin[c]	bilayer	bilayer	bilayer[e]	H_{II}

[a] In cases where bilayer and nonbilayer phases coexist, only the nature of the nonbilayer component is given. The isotropic phase is believed to represent a 'molten' cubic phase (see *15*). [b] From Killian et al. (*15*). [c] From Van Echteld et al. (*13*). [d] At a 1/7 ratio of peptide to lipid, a broad isotropic signal is observed (M. R. R. de Planque and J. A. Killian, unpublished observations). [e] System forms an inverse hexagonal phase at a 1/7 peptide/lipid ratio (*48*).

Effects of Mismatch on Chain Length As Compared with Effects on Phase Behavior. We previously found using ^{31}P NMR that WALP peptides at higher concentrations are capable of inducing nonbilayer phases, the nature of which depends on the particular WALP/PC combination chosen and thus on the precise extent of hydrophobic mismatch (*15*). The phase behavior of the peptide/lipid mixtures, used in this study, is summarized in Table 5. This offers a unique opportunity to relate the direct, ^2H NMR-derived length data to independent mismatch information from another technique. The induction of an inverse hexagonal lipid phase was ascribed to the WALP peptides being substantially too short when compared with the host bilayer (*15*). This would imply the existence of a lipid-shrinking potential in these systems when the peptide/lipid molar ratio is lowered such that the lipids are forced to remain in a bilayer, as in the present study. Similarly, a planar bilayer should accommodate approximately matching peptides and longer peptides, and the latter would have a lipid-stretching influence. Both expectations are consistent with the present results obtained on the WALP peptides, as can be seen from comparison of Tables 2 and 5. However, the lipid shrinking effect seems rather small as compared to the lipid stretching effect. Moreover, the induction of an isotropic lipid phase has been interpreted as the peptide being slightly too short (*15*), yet at the peptide concentrations used for ^2H NMR, in such systems either no effect or even a slight stretching of the lipids is observed. This apparent discrepancy might be explained by considering the physical nature of the peptide surface (*64*). In this view, the WALP peptides may be considered as a relatively 'hard' surface, as compared to the fluid acyl chains in the lipid bilayer. Therefore, they will give rise to a *general* increase in lipid chain order in all systems, independent of the extent of mismatch.

The effects of gramicidin on lipid chain order seem to deviate even more from the mismatch predictions based on lipid phase behavior. Gramicidin modulates lipid phase

behavior in much the same way as does WALP16 (for comparison, see *15* and *69*), implying a similar effective hydrophobic length. Yet for most lipid systems gramicidin influences bilayer thickness in a way similar to a longer WALP peptide. Gramicidin even causes a lipid stretch in DPPC, although at higher gramicidin concentrations a hexagonal phase is formed in this lipid system (*48*). This apparent discrepancy also may be explained by the physical nature of the surfaces of the peptides. The amino acid side chains of gramicidin in general are rather bulky and have relatively small spatial separations, due to its organization in a $\beta^{6.3}$ helix (Figure 6). The side chains of the α-helical WALP peptides are less tightly packed, also because there are fewer tryptophans and the protruding, and probably highly mobile, leucine side chains are separated by short alanine spacers. Therefore, gramicidin would offer a 'harder' lipid contact surface than do the WALP peptides, thereby increasing the chain order more than a WALP peptide with the same hydrophobic length in all lipid systems. This interpretation is consistent with the considerably smaller degree of motional restriction of the 14-SASL chain by the WALP peptides than by gramicidin that is observed by ESR.

Biological Significance. In the relatively large number of ^{2}H NMR studies that have been carried out on the influence of integral membrane proteins (for reviews, see *70*−*73*), it has generally been found that lipid chain order is not changed much by the presence of integral proteins, even at high concentrations. However, most of these experiments were carried out on lipid/protein systems that closely resembled biological membranes. On energetic grounds, Mouritsen and Bloom (*11*) anticipated a close match between biological bilayers and their natural integral membrane proteins, which could explain the small or negligible variations in lipid chain order upon protein incorporation.

The present findings, based on two-component systems consisting purely of a single lipid and a single peptide, both with well-defined variations in hydrophobic length and thus enabling the use of systems with a large difference in component hydrophobic length, do show a clear, mismatch-dependent response of the acyl chain order. Comparison of the ^{2}H NMR results with previous studies on polyleucines (*74*, *75*) reveals that the WALP peptides have the larger influence on mean membrane thickness. This is most directly demonstrated by the observation that a 24-residue-long peptide with a Leu_{20}-core, under similar experimental conditions, caused the same increase in quadrupolar splitting of the plateau region (*74*) as a WALP analogue with only 16 residues in total. Possible explanations for this difference may involve a larger tendency of the lysine-flanked polyleucines toward tilt or aggregation, which would reduce the extent of lipid stretching or the fraction of first-shell lipids. For the WALP peptides, no aggregation was observed. In this case, critical interactions between the lipids and the tryptophan indole rings could occur that inhibit oligomerization, because of the size of these aromatic residues, their shape, and/or their strong preference for a bilayer interface (*63*). Thus, our studies indicate that interfacially localized tryptophans may be important for determining the effects of mismatching proteins in biological membranes.

Even for the WALP peptide systems, however, the response of the lipids is relatively small and compensates at most only partially for the mismatch, suggesting either that such a partial mismatch configuration is allowed energetically or that other, additional responses occur. Thus, the results in this study suggest that also in biological membranes a large mismatch may not lead to significant stretching or shrinking of the acyl chains. This is supported by studies in *Acholeplasma laidlawii* (*76*), which showed that a variation of as much as 8 Å in bilayer thickness could be tolerated without an apparent effect of the proteins on acyl chain order. A likely alternative possibility to relieve mismatch effects in biological membranes is that the proteins become surrounded preferentially by the lipids with the best matching hydrophobic length (e.g. *5*, *77*). By such a mechanism, hydrophobic mismatch could promote the occurrence of preferential interactions of the type that may lead to lipid and protein sorting and domain formation (*3*, *4*, *6*).

Summarizing Conclusions. In summary, incorporation of WALP peptides in PC bilayers can induce a hydrophobic mismatch that perturbs the bilayer in a systematic manner without apparent peptide aggregation. In addition, a comparison of the relative effects of gramicidin and WALP peptides demonstrates that other factors, such as peptide shape, may modulate the effects of hydrophobic mismatch. However, in nearly all cases the adaptation of the lipids is insufficient to relieve the mismatch completely. It thus seems either that the system allows a partial mismatch configuration, as suggested by theoretical studies (*64*), or that other responses, such as peptide tilt or conformational adaptation, occur to achieve a more complete mismatch response (*7*, *8*). The WALP family of peptides represents an effective system for investigating these possibilities.

NOTE ADDED IN PROOF

After submission of this manuscript, a related study appeared on a 28-residue-long peptide with a Leu24 core (*80*). This lysine-flanked polyleucine peptide was incorporated in bilayers of 1-palmitoyl-2-oleoyl-*sn*-glycero-3-phosphocholine, up to concentrations of 9 mol %. From conventional and nonconventional ESR experiments, it was concluded that the peptide was highly miscible in these membranes and that it was primarily monomeric. This result supports our interpretation of the conventional ESR spectra that the WALP peptides are present as monomers or at most as dimers.

ACKNOWLEDGMENT

We thank Drs. Ben de Kruijff and Olaf Andersen for helpful suggestions on the manuscript, Drs. Vladimir and Mila Chupin for lipid acyl chain perdeuteration, and Frau B. Angerstein for spin-label synthesis.

REFERENCES

1. Johannsson, A., Smith, G. A., and Metcalfe, J. C. (1981) *Biochim. Biophys. Acta 641*, 416−421.
2. Montecucco, C., Smith, G. A., Dabbeni-sala, F., Johansson, A., Galante, Y. M., and Bisson, R. (1982) *FEBS Lett. 144*, 145−148.
3. Sperotto, M. M., and Mouritsen, O. G. (1993) *Eur. Biophys. J. 22*, 323−328.
4. Marsh, D. (1995) *Mol. Membr. Biol. 12*, 59−64.
5. Lehtonen, J. Y. A., and Kinnunen, P. K. J. (1997) *Biophys. J. 72*, 1247−1257.
6. Pelham, H. R., and Munro, S. (1993) *Cell 75*, 603−605.

7. Zhang, Y.-P., Lewis, R. N. A. H., Henry, G. D., Sykes, B. D., Hodges, R. S., and McElhaney, R. N. (1995a) *Biochemistry 34*, 2348−2361.
8. Zhang, Y.-P., Lewis, R. N. A. H., Hodges, R. S., and McElhaney, R. N. (1995b) *Biochemistry 34*, 2362−2371.
9. Ren, J., Wang, Z., and London, E. (1997) *Biochemistry 36*, 10213−10220.
10. Ryba, N. J. P., and Marsh, D. (1992) *Biochemistry 31*, 7511−7518.
11. Mouritsen, O. G., and Bloom, M. (1984) *Biophys. J. 46*, 141−153.
12. Owicki, J. C., Springgate, M. W., and McConnell, H. M. (1978) *Proc. Natl. Acad. Sci. U.S.A. 75*, 1616−1619.
13. Van Echteld, C. J. A., De Kruijff, B., Verkleij, A. J., Leunissen-Bijvelt, J., and De Gier, J. (1982) *Biochim. Biophys. Acta 692*, 126−138.
14. Killian, J. A., Prasad, K. U., Urry, D. W., and De Kruijff, B. (1989) *Biochim. Biophys. Acta 978*, 341−345.
15. Killian, J. A., Salemink, I., De Planque, M. R. R., Lindblom, G., Koeppe, R. E., II, and Greathouse, D. V. (1996) *Biochemistry 35*, 1037−1045.
16. Prosser, R. S., and Davis, J. H. (1992) *Biochemistry 31*, 9355−9363.
17. Zhang, Y.-P., Lewis, R. N. A. H., Hodges, R. S., and McElhaney, R. N. (1992) *Biochemistry 31*, 11579−11588.
18. Killian, J. A. (1992) *Biochim. Biophys. Acta 1113*, 391−425.
19. Landolt-Marticorena, C., Williams, K. A., Deber, C. M., and Reithmeier, R. A. F. (1993) *J. Mol. Biol. 229*, 602−608.
20. Henderson, R., Baldwin, J. M., Ceska, T. A., Zemlin, F., Beckman, E., and Downing, K. A. (1990) *J. Mol. Biol. 213*, 899−929.
21. Weiss, M. S., Abele, U., Weckesser, J., Welte, W., Schiltz, E., and Schultz, G. E. (1991) *Science 254*, 1627−1630.
22. Schiffer, M., Chang, C.-H., and Stevens, F. J. (1992) *Protein Eng. 5*, 213−214.
23. Wallin, E., Tsukihara, T., Yoshikawa, S., Von Heijne, G., and Elofsson, A. (1997) *Protein Sci. 6*, 808−815.
24. Boss, W. F., Kelley, C. J., and Landsberger, F. R. (1975) *Anal. Biochem. 64*, 289−292.
25. Hermetter, A., and Paltauf, F. (1983) in *Ether Lipids. Biochemical and Biomedical Aspects* (Mangold, H. K., and Paltauf, F., Eds.) p 415, Academic Press, New York.
26. Hubbell, W. L., and McConnell, H. M. (1971) *J. Am. Chem. Soc. 93*, 314−326.
27. Davis, J. H., Jeffrey, K. R., Bloom, M., Valic, M. I., and Higgs, T. P. (1976) *Chem. Phys. Lett. 42*, 390−394.
28. Seelig, A., and Seelig, J. (1977) *Biochemistry 16*, 45−50.
29. Schäfer, H., Mädler, B., and Volke, F. (1995) *J. Magn. Reson. A 116*, 145−149.
30. Burnett, L. J., and Muller, B. H. (1971) *J. Chem. Phys. 55*, 5829−5831.
31. Seelig, J., and Niederberger, W. (1974) *J. Am. Chem. Soc. 96*, 2069−2072.
32. Stockton, G. W., Polnaszek, C. F., Tulloch, A. P., Hasan, F., and Smith, I. C. P. (1976) *Biochemistry 15*, 954−966.
33. Lafleur, M., Fine, B., Sternin, E., Cullis, P. R., and Bloom, M. (1989) *Biophys. J. 56*, 1037−1041.
34. Bouchard, M., Boudreau, N., and Auger, M. (1996) *Biochim. Biophys. Acta 1282*, 233−239.
35. Seelig, A., and Seelig, J. (1974) *Biochemistry 13*, 4839−4845.
36. Bloom, M., and Mouritsen, O. G. (1988) *Can. J. Chem. 66*, 706−712.
37. Nagle, J. F. (1993) *Biophys. J. 64*, 1476−1481.
38. Elder, M., Hitchcock, P., Mason, R., and Shipley, G. G. (1977) *Proc. R. Soc. London A 354*, 157−170.
39. Koenig, B. W., Strey, H. H., and Gawrisch, K. (1997) *Biophys. J. 73*, 1954−1966.
40. Davis, J. H. (1983) *Biochim. Biophys. Acta 737*, 117−171.
41. Pauls, K. P., MacKay, A. L., and Bloom, M. (1983) *Biochemistry 22*, 6101−6109.
42. Bonev, B., and Morrow, M. R. (1996) *Biophys. J. 70*, 2727−2735.
43. Oldfield, E., Meadows, M., Rice, D., and Jacobs, R. (1978) *Biochemistry 17*, 2727−2740.
44. Seelig, A., and Seelig, J. (1975) *Biochim. Biophys. Acta 406*, 1−5.
45. Douliez, J.-P., Léonard, A., and Dufourc, E. J. (1995) *Biophys. J. 68*, 1727−1739.
46. Sankaram, M. B., and Thompson, T. E. (1990) *Biochemistry 29*, 10676−10684.
47. Rice, D., and Oldfield, E. (1979) *Biochemistry 18*, 3272−3279.
48. Watnick, P. I., Chan, S. I., and Dea, P. (1990) *Biochemistry 29*, 6215−6221.
49. Lewis, B. A., and Engelman, D. M. (1983) *J. Mol. Biol. 166*, 211−217.
50. Sperotto, M. M., and Mouritsen, O. G. (1988) *Eur. Biophys. J. 16*, 1−10.
51. Marsh, D. (1981) in *Membrane Spectroscopy. Molecular Biology, Biochemistry and Biophysics* (Grell, E., Ed.) Vol. 31, pp 51−142, Springer-Verlag, Berlin, Heidelberg, and New York.
52. Marsh, D. (1993) in *New Comprehensive Biochemistry, Protein−Lipid Interactions* (Watts, A., Ed.) Vol. 25, pp 41−66, Elsevier, Amsterdam.
53. Marsh, D. (1997) *Eur. Biophys. J. 26*, 203−208.
54. Marsh, D. (1985) in *Progress in protein−lipid interactions* (Watts, A., and De Pont, J. J. H. H. M., Eds.) Vol. 1, pp 143−172, Elsevier, Amsterdam.
55. Marsh, D., and Horváth, L. I. (1997) *Biochim. Biophys. Acta* (in press).
56. Chapman, D., Cornell, B. A., Eliasz, A. W., and Perry, A. (1977) *J. Mol. Biol. 113*, 517−538.
57. Cornell, B. A., Sacré, M. M., Peel, W. E., and Chapman, D. (1978) *FEBS Lett. 90*, 29−35.
58. Ge, M., and Freed, J. H. (1993) *Biophys. J. 65*, 2106−2123.
59. Lange, A., Marsh, D., Wassmer, K.-H., Meier, P., and Kothe, G. (1985) *Biochemistry 24*, 4384−4392.
60. Moser, M., Marsh, D., Meier, P., Wassmer, K.-H., and Kothe, G. (1989) *Biophys. J. 55*, 111−123.
61. Evans, E. A., and Needham, D. (1987) *J. Phys. Chem. 91*, 4219−4228.
62. Mouritsen, O. G., and Bloom, M. (1993) *Annu. Rev. Biophys. Biomol. Struct. 22*, 145−171.
63. Wimley, W. C., and White, S. H. (1996) *Nat. Struct. Biol. 3*, 842−848.
64. Fattal, D. R., and Ben-Shaul, A. (1993) *Biophys. J. 65*, 1795−1809.
65. Piknová, B., Pérochon, E., and Tocanne, J.-F. (1993) *Eur. J. Biochem. 218*, 385−396.
66. Goulian, M., Mesquita, O. N., Fygenson, D. K., Nielsen, C., Andersen, O. S., and Libchaber, A. (1998) *Biophys. J. 74*, 328−337.
67. Cornea, R. L., Jones, L. R., Autry, J. M., and Thomas, D. D. (1997) *Biochemistry 36*, 2960−2967.
68. Pérez-Gil, J., Casals, C., and Marsh, D. (1995) *Biochemistry 34*, 3964−3971.
69. Killian, J. A., Burger, K. N. J., and De Kruijff, B. (1987) *Biochim. Biophys. Acta 897*, 269−284.
70. Seelig, J., and Seelig, A. (1980) *Q. Rev. Biophys. 13*, 19−61.
71. Jacobs, R. E., and Oldfield, E. (1981) *Prog. NMR Spectrosc. 14*, 113−136.
72. Devaux, P. F., and Seigneuret, M. (1983) in *Biological Magnetic Resonance* (Berliner, L. J., and Reuben, J., Eds.) Vol. V, pp 183−299, Plenum Press, New York.
73. Bloom, M., and Smith, I. C. P. (1985) in *Progress in Protein−Lipid Interactions* (Watts, A., and De Pont, J. J. H. H. M., Eds.) pp 61−88, Elsevier, Amsterdam.
74. Roux, M., Neumann, J.-M., Hodges, R. S., Devaux, P. F., and Bloom, M. (1989) *Biochemistry 28*, 2313−2321.
75. Nezil, F. A., and Bloom, M. (1992) *Biophys. J. 61*, 1176−1183.
76. Thurmond, R. L., Niemi, A. R., Lindblom, G., Wieslander, Å., and Rilfors, L. (1994) *Biochemistry 33*, 13178−13188.
77. Dumas, F., Sperotto, M. M., Lebrun, M.-C., Tocanne, J.-F., and Mouritsen, O. G. (1997) *Biophys. J. 73*, 1940−1953.

78. Arseniev, A. S., Lomize, A. L., Barsukov, I. L., and Bystrov, V. F. (1996) *Biol. Membr. 3*, 1077−1104.

79. Ketchem, R. R., Hu, W., and Cross, T. A. (1993) *Science 261*, 1457−1460.

80. Subczynski, W. K., Lewis, R. N. A. H., McElhaney, R. N., Hodges, R. S., Hyde, J. S., and Kusumi, A. (1998) *Biochemistry 37*, 3156−3164.

BI980233R